

An Adiabatic Calorimeter for High-resolution Heat Capacity Measurements in the Temperature Range from 12 to 300 K

Masami TATSUMI, Takasuke MATSUO, Hiroshi SUGA, and Syüzô SEKI

Department of Chemistry, Faculty of Science, Osaka University, Toyonaka, Osaka 560

(Received May 23, 1975)

Construction of a high resolution calorimeter of an adiabatic type for single crystals is described. It uses a bank of thermistors for high resolution measurements in addition to a miniature platinum resistance thermometer. The results of heat-capacity measurements on benzoic acid as a standard material showed the inaccuracy of $\pm 0.1\%$ and the imprecision was confirmed to be less than $\pm 0.05\%$ between 50 and 275 K.

Singularities observed in thermodynamic properties of a substance at the critical point are characterized by the quantities known as the critical exponents. These quantities are of paramount importance in the study of critical phenomena and their determination as well as verification of various relation expected to hold among them are central problems of experimental and theoretical investigations in this field.^{1,2)} Elucidation of the nature of a phase transition by determining reliable values of the critical exponents requires measurement of the thermodynamic quantities with high resolution both in the independent variable (particularly, the temperature) and in the quantity measured. Although the heat capacity exponents have been evaluated for a number of substances, lack of sufficient resolution in the measurement diminishes their reliability in a large number of cases. Among the notable exception in this respect is the excellent high resolution heat capacity measurement performed by Buckingham, Fairbank and Keller³⁾ on the λ -transition in liquid ^4He . Other critical phase transitions which have been studied include those in magnetic and dielectric substances and binary liquid mixtures.^{4–10)} As to the dielectric transitions, with which we are concerned mainly, reliable high resolution heat capacity data are deplorably limited in number and in the substance dealt with.

There are two types of calorimeter used for high-resolution measurement which operate on different principles. One is the discontinuous heating method (the DC method) and the other the stationary state method (the AC method).¹¹⁾ We adopted the DC method, in view of the problem of the present interest. Although the AC method has desirable features that the measurements can be made with smaller amount of the sample and easily operated automatically, it has the demerits: the specimens to be studied are limited to non-volatile substances and the absolute values of the heat capacities are very difficult to determine. On the other hand, the DC method has no restrictions on specimens and yields the absolute value of heat capacities and is able to detect a minute 1-st order component which sometimes accompany the critical point. This last possibility is also important for characterization of the phase transition phenomenon.

This paper describes an adiabatic-type high-resolution calorimeter which works in the temperature range between 12 and 300 K. The accuracy of this apparatus was determined by the measurement of heat capacities

of benzoic acid. The results¹²⁾ of the high resolution measurement on the single crystal of $\text{SnCl}_2 \cdot 2\text{H}_2\text{O}$ revealed the reliability of this apparatus.

Experimental

Construction of Apparatus. The calorimeter consists of four major parts, viz., the cryostat, the adiabatic-control circuit, the temperature-measuring circuits and the energy supply and its measuring circuit (Fig. 1). A special feature of the apparatus is that it is equipped with two thermometers, a platinum resistance thermometer and a thermistor thermometer. The former provides an accurate temperature scale based on the International Practical Temperature Scale 1968, while the latter enables precise measurement of small temperature increment of the calorimeter. The platinum resistance thermometer is also used for calibrating the thermistor. This feature endows the apparatus with a unique capability of measuring the heat capacity with high accuracy and precision. Details of the calorimeter design and construction are described in the following.

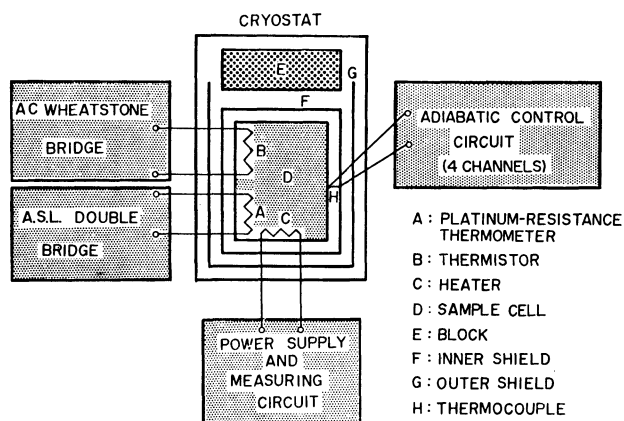


Fig. 1. Block diagram of the calorimetric system.

1) Cryostat. Figure 2 shows a schematic drawing of the cryostat. The calorimeter cell (A), whose detailed construction is given below, is suspended in the inner adiabatic jacket (B) with a 0.5 mm thick nylon cord at the top. Its horizontal position relative to the jacket is adjusted to the center of the jacket with three thinner nylon cords attached at the bottom of the cell. The inner jacket of a thin copper shell of 0.5 mm thickness consists of three parts, i.e., a cylinder, upper cone (these two weighing 114 g) and a bottom cone (22 g). The bottom cone is firmly attached to the cylinder with three pairs of screw. The temperature of the inner

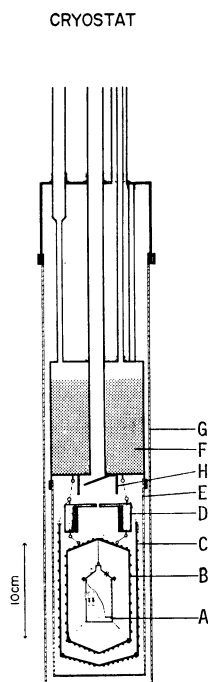


Fig. 2. Sectional view of the cryostat

A, Sample cell; B, Inner jacket; C, Outer jacket;
D, Block; E, Inner vacuum can; F, Coolant container;
G, Outer vacuum can; H, Sleeve

jacket is controlled relative to that of the cell. The outer jacket (C) is also a temperature-regulated copper cylinder (275 g) whose function is to prompt establishment of the adiabatic condition of the cell by keeping a stabilized temperature difference between the inner jacket and itself. The copper block (D) is a temperature-controlled heat reservoir, which helps the inner jacket to work correctly by tempering the thermal agitation coming down through the leads. The block has a large mass for this purpose and a copper bobbin for winding the heater wires. These three temperature-controlled components are suspended in the inner vacuum can (E) from the bottom of the coolant container (F). The latter is surrounded by the outer vacuum can (G) which is normally immersed in an appropriate coolant, usually liquid nitrogen or methanol-dry ice mixture according to the temperature region being studied.

The leads for the thermometers, heaters, and thermocouples are tightly wound around the inner jacket and the block, and then around the sleeve (H) attached to the bottoms of the inner coolant container in turn and finally led out through a Dekhochinsky seal and a glass-hermetic seal. The lead wires to the calorimeter cell are connected with terminals insulated by teflon attached to the inner jacket. The spaces in the inner can and between the inner and the outer can are evacuated independently to *ca.* 0.2 mPa by an oil vacuum pump.

2) *Calorimeter Cell.* The calorimeter cell for the samples of single crystals is shown schematically in Fig. 3. This is a chromium-plated copper cylinder, about 30 mm in diameter and 60 mm long with the wall 0.3 mm thick.

A dismountable lid on the top end of the cell allowed loading it with a large snugly-fitting single crystal. The vacuum-tight closure was achieved by applying a thin layer of Apiezon N grease between the lapped faces of the flanges of the cylinder and the lid and fixing them tightly together with eight pairs of screw. An indium O-ring with 0.5 mm

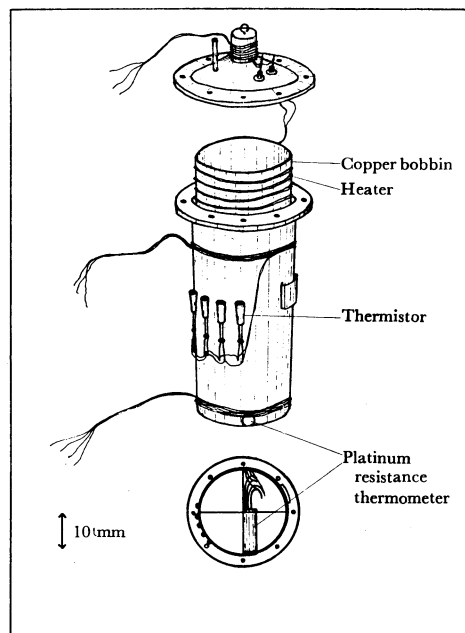


Fig. 3. Sketch of the calorimeter cell for single crystals.
The bobbin is slightly lifted for better illustration.

diameter can also be used. This closure could hold cell at 0.1 mPa. The two types of thermometers are attached to the outside of the cell. One is a miniature platinum-resistance thermometer (Model S 1059, the Minco Products, USA). It is 13 mm long and 3 mm in diameter and has a nominal resistance 100 Ω at 0 $^{\circ}\text{C}$. It is placed in a closely fitting copper tube soldered on the bottom face of the cell. The other is a bank of five glass-bead thermistors (Shibaura Denshi, model NSB) for the high resolution measurements. The glass beads were wrapped in a small piece of thin copper sheet, and soldered on the side of the cell side by side. Nominal resistance of each of the thermistor is 4 k Ω at 0 $^{\circ}\text{C}$ and 0.13 k Ω at 100 $^{\circ}\text{C}$. The connection of the five thermistors was changed so as to obtain the resultant resistance of 10–20 k Ω in the temperature interval of interest. This cell had a copper bobbin, 0.2 mm thick and of a slightly smaller diameter than the inner diameter of the cell itself. On this bobbin the calorimeter heater was wound bifilarly and cemented in place with GE adhesive. The heater wire was double silk wrapped constantan (Driver & Harris AWG No. 36) with total resistance of 100 Ω . The primary role of the bobbin is to promote temperature homogeneity in the cell during the heat-on period. Helium gas for improving thermal conduction within the sample space could be admitted before seal-off.

3) *Adiabatic Control.* The heat-transfers between calorimeter cell and its environment may be caused by three factors, that is, the convective heat leak which was eliminated by maintaining vacuum in the calorimeter system, the radiative heat transfer and the heat transfer by conduction along the leads bundle. As regards the radiative heat transfer it was reduced by gold-plating the inner surface of the radiation jacket and chromium-plating the outer surface of the calorimeter cell to obtain high reflectivity. To minimize the heat transfer by conduction, the leads to the calorimeter cell must be as thin as possible, but it is in conflict with the requirement of high electric conductivity of leads. To minimize heat exchange by the second- and third-mentioned mechanisms, the temperature of the inner jacket, about which leads were wound tightly, must be equalized to that of the

outer surface of the calorimeter cell, and especially to minimize the temperature gradient along both surfaces is required in order to reduce the radiation heat transfer. Temperatures of the bottom cone and other part of the inner jacket are controlled separately. The resistances of the heater wires were adjusted so as to make the power dissipation in the side and cone proportional to their respective mass (cylinder, uppercone 100 Ω and bottom cone 50 Ω). Thermocouples (Chromel P-constantan) were attached at five locations on the inside and outside of the cylinder and at three locations on the bottom cone. The two thermocouples insulated by cellophane adhesive tape were covered with small thin phosphor bronze plates which were attached to the inner bottom cone with two screws. These thermocouples detect temperature difference between the cell and the side and between the cell and the bottom of the adiabatic jacket. During a test run of the apparatus, it was found that the thermal conductivity between the inner and outer jackets was so small that the inner jacket, especially its bottom was liable to over-heat. It was remedied by linking thermally the bottoms of the two jackets with copper wire of appropriate length and diameter. The thermocouples (Chromel P-constantan) sense the temperature differences between the block and the inner jacket and between the outer jacket and the inner jacket, and the currents flow through the heater of the block (200 Ω) and the outer jacket (197 Ω). The temperatures of the block and the outer jacket were usually maintained lower than that of the inner jacket by several kelvin. On-off type of the regulator action, even if it is satisfactory in regard to the stability of the regulation, would cause strong noise in the thermometer circuits to the point of saturating the detectors. This difficulty was overcome by proportional mode of action which regulates the input power to the jacket heater smoothly in proportional to the temperature imbalance. The control system only with the proportional function could not automatically follow the temperature variation of the calorimeter cell at the early stage of and immediately after the heating period. Therefore, the off-set voltages, which were determined at an equilibration and a heating periods respectively, had to be readjusted quickly. To reduce the labor of paying attention to the off-set signal indicators, an integral action was added to the proportional action. In this improved regulator system (Fig. 4) the thermocouple voltage was measured and amplified with DC microvoltmeter (Keithley model 149), the output of which was fed into the proportional-integrating circuit as an error signal, and drove the jacket heater. The

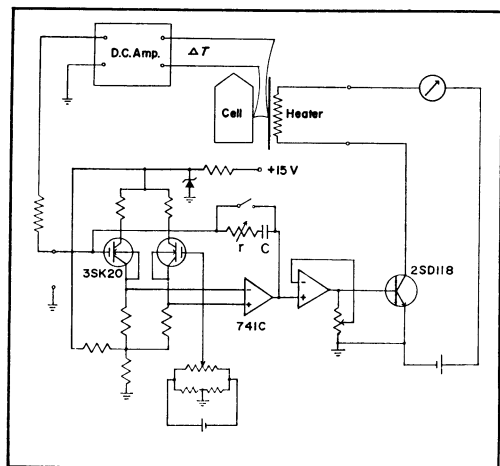


Fig. 4. Electric proportioning-integrating circuit.

heater current was normally less than 50 mA. By using this circuit the temperature difference between the inner jacket and the calorimeter cell was less than 0.5 mK during both equilibration and heating periods.

4) *Measurements of the Temperature.* a) *Circuit System for the Platinum Resistance Thermometer:* The miniature platinum resistance thermometer was used as a temperature sensor which determined the absolute temperature scale. The precision AC double bridge (Automatic System Laboratory Inc. Model H8) with inductively coupled ratio arms was used to measure the thermometer resistance. This bridge has the merit that it requires only one balancing operation, since use of alternating current eliminates the effect of thermal emf's. However, some care had to be paid to the characteristics of the apparatus on using it in low temperature calorimeter, as will be described below. The basic circuit of this bridge is shown in Fig. 5 which, for the sake of clarity, does not contain

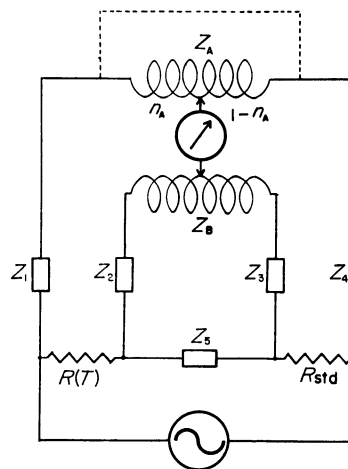


Fig. 5. Basic circuit of the ASL AC double bridge.

any phase balancing component. $R(T)$ is a resistance of the thermometer, R_{std} is a resistance of the standard resistor and Z_1 , Z_2 , Z_3 , Z_4 , and Z_5 represent lead impedances. Z_A and Z_B are impedance of the inductive ratio arms which have $4 \times 10^5 \Omega$ at 390 Hz and n_A and n_B the ratios of the arms. The equation of the balance which is that of the Kelvin double bridge is given precisely by

$$R(T) = R_{std} \left[\frac{n_A Z_A + Z_1}{(1 - n_A) Z_A + Z_4} + Z_5 \frac{(1 - n_B) Z_B + Z_3}{Z_B + Z_2 + Z_3 + Z_5} \right. \\ \left. \times \frac{n_A Z_A + Z_1}{(1 - n_A) Z_A + Z_4} - \frac{n_B Z_B + Z_3}{(1 - n_B) Z_B + Z_3} \right]. \quad (1)$$

In this bridge $Z_A = Z_B$, $Z_1 = Z_2$, $Z_3 = Z_4$ and Z_A and Z_B are much larger than Z_1 , Z_2 , Z_3 , Z_4 , and Z_5 , so if n_A and n_B are not close to unity or zero, this equation is simplified as given below,

$$R(T) = R_{std} \frac{n_A}{1 - n_A} \left[1 + \frac{Z_1}{n_A Z_A} - \frac{Z_4}{(1 - n_A) Z_A} \right]. \quad (2)$$

If ultimately high-precision measurement of the resistance is required, the ratio n_A must lie between 0.2 and 0.8, so the value of the standard resistor has to be varied in accordance with the resistance of the thermometer. For this purpose, three standard resistors (100 Ω , 6.238453 Ω , 0.390430 Ω) were prepared and kept in the box thermostated within ± 0.03 K.

Three corrections had to be made in the measurements by using this AC double bridge. The first was correction for eliminating the effects of the impedance of the leads. If Z_1 and Z_4 were much smaller than Z_A , the last two terms in Eq. (2) were neglected, so Eq. (2) becomes to be $R(T) = R_{std} n_A / (1 -$

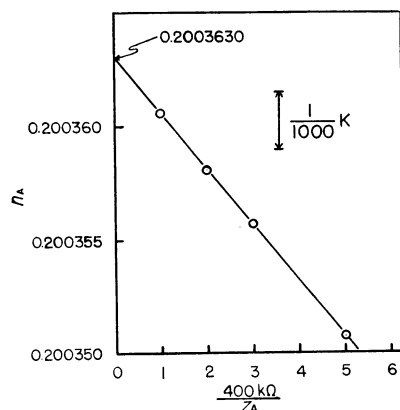


Fig. 6. Correction for the impedance of the leads to the platinum resistance thermometer.

n_A). But the condition $Z_A \gg Z_1$, Z_4 is not always satisfied because the thermometer-lead impedance could not be reduced below a few ohms. The correction for this effect was achieved by connecting resistors in parallel with Z_A in turn, which is indicated by the dashed lines in Fig. 5. The " n_A " are plotted against the $400/(\text{resultant resistance})$ in Fig. 6. Extrapolation of this straight line to the infinite resultant resistance gives the corrected n_A . This means that, since no current flows in this circuit because of its infinite resistance, the voltage drop due to Z_1 does not occur, so the extrapolated n_A corresponds to that which would be obtained if Z_1 is zero. The slope of this straight line increases with increasing $R(T)$ and R_{std} . The magnitude of this correction was less than $3/1000$ K at any temperature range studied. The second correction is concerned with the self-heating of the thermometer. Since the Minco thermometer has the higher resistance and smaller volume than the platinum resistor of normal type, the effect of self-heating due to the current flow for measurements could not be neglected. This effect could be eliminated, however, in the following manner. A set of measurements with various bridge carrier voltages was plotted against the power dissipated in the thermometer and the n_A at the zero power dissipation was determined by extrapolation. This n_A value corresponds to that measured at condition where no current flowed in the thermometer. In actual heat capacity measurements, the power dissipation in the thermometer was typically $5 \mu\text{W}$. The third correction, *i.e.*, the effect of the inductance of the thermometer element is not quite clear. The inductance of the Minco thermometer ($\sim 30 \mu\text{H}$) is considerably larger than that of the typical L & N Pt-thermometer ($\sim 1.5 \mu\text{H}$). Therefore, the DC resistance and the apparent AC resistance of the Minco thermometer can possibly be appreciably different from each other. This possible effect was taken into account by making the calibration of the Minco thermometer at a fixed frequency (390 Hz), while the standard thermometer (L & N Pt-resistor) was measured with DC current. The calibration table is given in the apparent resistance of the Minco thermometer against temperature. In principle, the calibration may have been performed at several frequencies to determine the DC resistance by extrapolation, but it was impracticable because of the instrumental limitation. This caused no inconvenience because the Minco thermometer was always used in conjunction with the ASL AC double bridge at the fixed carrier frequency.

b) *Calibration of the Platinum Resistance Thermometer:* The Minco platinum resistance thermometer was calibrated against the standard capsule type Leeds & Northrup Pt-thermometer which was recalibrated according to the IPTS-68. Two

thermometers were mounted side by side in the well drilled in a copper block and set in the cryostat. The resistance of the standard thermometer was measured with the DC Müller bridge (Leeds & Northrup 8071-B Type G-3), while that of the Minco thermometer by the AC bridge mentioned above. The calibration was carried out at the eight temperatures from 13.81 to 373.15 K. Three measurements were made at each of the internationally defined fix points: *i.e.*, the triple and boiling points of equilibrium H_2 , O_2 , H_2O , equilibrium H_2 at 25/76 atm and the boiling point of Ne. The accurate values of resistance for the Minco thermometer at these fixed points were determined by interpolation. The temperature determined from the calibration table of the standard thermometer and the resistances of the Minco thermometer were corrected according to the procedure described above.

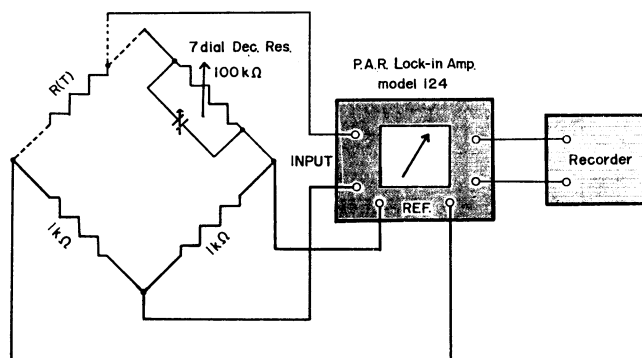


Fig. 7. AC Wheatstone bridge for the thermistor thermometer.

c) *Circuit System for the Thermistor Resistance Measurement:*

Figure 7 shows the AC Wheatstone bridge for the thermistors which was used in the high resolution measurements. A lock-in amplifier (Princeton Applied Research Corp. Model 124) was employed as a high sensitivity detector. The balance of the resistive and the reactive components could be performed easily. The variable air-capacitor connected in parallel with decade resistor was used in balancing a reactive component. The fixed-arm resistors and the seven dial decade resistor box were kept in an air thermostat. Each dial of the decade resistor was calibrated against the $10 \text{ k}\Omega$ standard resistor by the decade-for-decade method. The leads of the thermistor represented by the dashed lines in Fig. 7 have the same length so as to compensate their impedance effects. Induction noises to the thermometer leads were reduced by twisting the lead wires with each other. All the other lead wires (for the thermocouples and heaters, which were potential noise sources) were also twisted in go-and-return pairs with different pitches.

d) *Calibration of the Thermistor:* The thermistor was calibrated against the Minco platinum thermometer (IPTS-68) at each measurement. On determining the relation between the temperature scale and the resistance of the thermistor, the equation $T = \sum_{i=1}^n A^i (\ln R)^i$ ($n=2,3$ or 4)

was assumed and the expansion coefficients were determined by the least square fit. The deviations of the observed values from this equation were found to be less than $1 \times 10^{-3} \text{ K}$, which was precise enough to determine absolute temperatures by means of this method (Fig. 8).

5) *Circuit System for Energy Supply.* The power supply and measuring circuit is shown in Fig. 9. A constant voltage circuit was used for the power supply and a digital voltmeter (Takeda Riken Model TR-6515D) for the measurements of

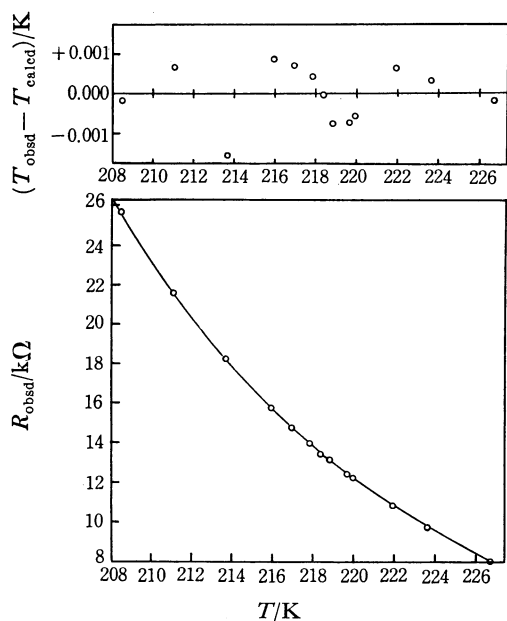


Fig. 8. Relation between the temperature and the net resistance of the five thermistors connected in parallel (lower), and the deviation of the calibration points from this curve (upper).

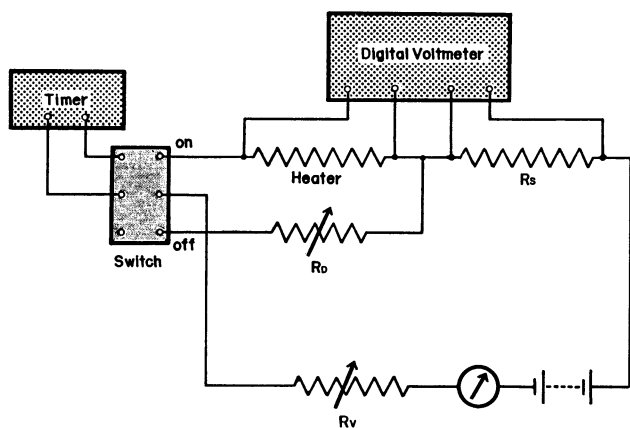


Fig. 9. Power supply and measuring circuit.

the current and voltage. The duration of the heat-on period was measured with a digital multifunction counter (Takeda Riken Model TR-5104). When the switch was put in position "on," the current start to flow through the calorimeter heater and counting of the timer begins. The current through the heater was determined by measuring the potential difference across the standard resistance R_s (100 Ω). A dummy resistor provided a by-pass circuit for the heater current. This device stabilized the out-put of the power supply when the calorimeter heater was switched off.

Results and Discussion

Determination of Heat Capacity of Benzoic Acid.

The measurements and calculations of the gross heat capacity were carried out as follows. After the initial temperature T_i ; i.e. the steady state temperature before heating, was measured, the electrical energy Q was introduced into the calorimeter. When the equilibrium state was confirmed after switching the heater current off, the

final temperature T_f was determined. The steady state temperatures T_i and T_f were determined by following the temperature drifts as a function of time. If the natural drifts due to the imperfection of the adiabatic regulation were present, an additional corrections would be required. The electrical energy Q was determined as the product of the average calorimeter heater voltage \bar{e} , the current i , and the time interval t , of the applied power input: i.e. $Q = \bar{e}it$. From the knowledge of these quantities, the gross heat capacity was determined by the equation: $Q/(T_f - T_i)$ at the mean temperature $(T_i + T_f)/2$. In the case of the high resolution measurements, the adiabatic regulation was strictly adjusted in order to eliminate the temperature drift for a long time. The precise determination of the heat capacity employing the small temperature increment is more liable to be affected by the heat leak. The thermistor was calibrated over the range of about 30 K including the temperature interval of the high-resolution measurement. The heat capacity is given by the equation, $C = Q/(dT/dR)_{T=T_{av}} \Delta R$, where $T_{av} = \{T(R_f) + T(R_i)\}/2$ and $\Delta R = |R_f - R_i|$. This calculation was performed on NEAC 2200 Model 700. In order to ascertain the over-all accuracy of the whole apparatus, the heat capacity measurement was performed on the benzoic acid as standard material which was prepared by the US National Bureau of Standards. The weight of the sample was 12.6106 g. The experimental values of the molar heat capacity are given in Table 1. Fig. 10 shows the deviation plots of our individual data points from the smoothed heat capacity of benzoic acid recommended by the US Calorimetry Conference.¹³⁾ The data by Furukawa *et al.*¹⁴⁾ and Cole *et al.*¹⁵⁾ are also plotted. These data were originally based on the IPTS-48, while our measurements were performed on the basis of the new temperature scale (IPTS-68). In order to compare these data with ours, they were converted into IPTS-68.¹⁶⁾

Deviation of our heat capacity data from the smoothed curve is about 1% of the total heat capacity at 20 K, 0.5% between 25 and 50 K ($\Delta T \approx 1.5$ K) and 0.1%

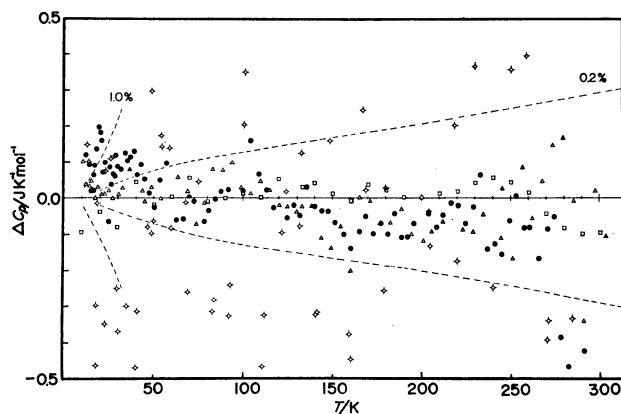


Fig. 10. Deviation plot of the measured values for the heat capacity of benzoic acid. ● the present data; □ Furukawa *et al.*; △ Cole *et al.*; ◇ Gorbunov *et al.* The abscissa is a statistical-smoothed-value of the data of several authors which include the results of Furukawa *et al.* and Cole *et al.*

TABLE 1. HEAT CAPACITY OF BENZOIC ACID

T K	C_p $\text{JK}^{-1}\text{mol}^{-1}$	T K	C_p $\text{JK}^{-1}\text{mol}^{-1}$	T K	C_p $\text{JK}^{-1}\text{mol}^{-1}$	T K	C_p $\text{JK}^{-1}\text{mol}^{-1}$
12.51	3.95	35.54	27.65	113.15	68.98	212.85	108.27
14.17	5.29	37.32	29.34	117.14	70.42	217.04	110.11
15.54	6.47	39.16	31.02	124.85	73.27	221.17	111.90
16.63	7.58	41.12	32.67	128.59	74.70	225.27	113.64
17.56	8.55	43.19	34.43	132.28	76.04	229.31	115.46
18.38	9.44	45.34	36.12	135.99	77.52	233.34	117.33
19.14	10.27	47.82	38.00	140.02	78.98	237.31	118.89
19.82	11.04	50.61	39.96	143.91	80.44	241.39	120.73
20.47	11.73	53.56	42.03	147.73	81.89	245.57	122.58
21.12	12.42	56.72	44.07	151.81	83.42	249.73	124.55
21.87	13.22	60.18	46.17	156.14	85.06	253.86	126.50
22.64	14.01	63.66	47.89	160.41	86.68	257.93	128.27
23.36	14.83	66.93	49.62	164.62	88.37	261.97	130.13
24.16	15.76	70.03	51.23	168.78	90.06	265.98	131.89
25.05	16.55	72.99	52.65	172.89	91.65	270.10	133.89
25.89	17.65	75.82	54.00	176.94	93.30	274.17	135.80
26.70	18.48	78.56	55.14	180.96	94.90	278.22	137.34
27.50	19.38	81.20	56.32	184.91	96.57	282.56	139.26
28.24	20.18	84.19	57.62	188.83	98.11	287.00	141.23
28.96	21.01	87.89	59.14	192.71	99.71	291.24	143.35
29.90	21.97	91.87	60.77	196.56	101.35	295.44	145.22
31.18	23.23	100.55	64.19	200.36	102.84	299.62	147.07
32.54	24.68	104.86	65.98	204.39	104.67	303.75	148.97
33.95	26.13	109.09	67.49	208.65	106.44		

between 50 and 275 K ($\Delta T \approx 4$ K). It should be noted that the weight of the samples employed by the different authors are considerably different, *i.e.*, 12.6106 g (ours), 100.99 g (Cole *et al.*) and 6.16 g ((Gorbunov *et al.*).¹⁷) Taking into account of the dependence of the precision of the measurement on the amount of the samples, our data are quite satisfying.

Sources of Inaccuracy in the Measurement. Next, we consider two aspects of the errors, namely, the systematic error (contributing to inaccuracy) and the random error (contributing to imprecision). A measure of the former is the deviation of the smoothed curve from the (unknown) "true" heat capacity, while the latter appears as the scattering of the data points about the smoothed curve. Several factors contribute to these errors; *i.e.*, errors in determination of the input energy and temperature and those due to the heat leak. The calorimeter heater voltage and current were determined to within 10 parts per million and the time interval within 1 ppm. Thus the errors due to the energy measurement are not a decisive factors in both the inaccuracy and the imprecision. The deviation of the thermometer calibration from the IPTS-68 was typically 4 mK and varied smoothly with temperature. The inaccuracy of the heat capacity due to the error in the temperature scale was estimated to be 0.3% at the lowest temperature and less than 0.02% at 200 K. The resistance resolution by the ASL bridge was better than $1 \times 10^{-5} \Omega$ which corresponds to 2.3×10^{-4} K at 15 K. At the higher temperatures, the temperature resolution is better than 1×10^{-4} K. Thus, the temperature measurement is not the largest source of the imprecision of the observed heat capacity, provided that

the temperature step for one measurement is not too small (1~3 K). The main factor contributing to the imprecision appears to be the heat leak to or from the sample cell. It is caused by transient deviation from the ideal adiabatic condition as well as by any stray emf in the difference-thermocouple circuits. The adiabatic condition in the equilibration period is achieved by eliminating the temperature change of the sample cell. This was done by adjusting the zero shifting emf at the input circuit of the DC micro-voltmeter so as to cancel the stray emf in the thermocouple leads, the resultant zero drift rate being taken as the indication of the optimum condition. Once adjusted suitably, the constant zero shifting emf served over a reasonably long series of measurements. If undisturbed, the adiabatic control system can keep the temperature of the sample cell constant within 0.3 mK for 24 hr at the desired temperature. The apparent temperature difference between the cell and the inner jacket was regulated to less than 0.5 mK during heating period. But this temperature difference does not take into account the possible temperature gradient along the surface of the cell and the inner jacket. Error due to this effect is difficult to estimate. But one of the method for its estimation would be to compare the heat capacity data obtained by different heating rates. This has not been done yet with the present calorimeter. At present, the temperature gradient effect and the stray emf, especially its variation with time, seems to be the most important factors limiting the precision of the measurement. In the high resolution measurement, the principle and procedure of the operation are essentially the same as in the ordinary measurement discussed

above, but more ingenuity and experience are required for successful operation because of the small temperature steps (two orders of magnitude smaller than in the ordinary measurements). The temperature was measured by the AC Wheatstone bridge with the imprecision less than 5×10^{-6} K. The heat leak during the equilibration period was minimized by optimizing the zero shifting emf in the difference-thermocouple circuits of the adiabatic jacket as mentioned above. This was done at the beginning of a series of measurements to within a drift rate $\pm 2 \mu\text{K}$ for at least 30 min. This procedure was facilitated by displaying the out-put signal of the null detector (P.A.R. model 124 lock-in-amplifier) of the bridge. Heat leak during the heating is again difficult to estimate, but it is believed to be less significant than in the ordinary measurement because the lower heater power disturbs the thermal uniformity of the jacket to the lesser extent. The relatively short heating period (60~100 s) is also an advantageous factor in this respect. Figure 11 shows an example of the recorder trace of the

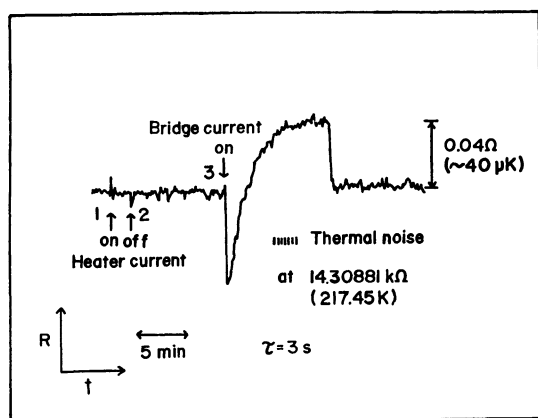


Fig. 11. An example of the high resolution measurement at 217.45 K.

R : the resistance of the thermistors.

t : the time.

τ : the time constant of the lock-in amplifier.

output signal (at 217.45 K) of the bridge null detector. The temperature remains constant within $5 \mu\text{K}$ after settling in the equilibrium value. It should be noted that the thermal noise from the thermistor calculated by the Nyquist formula corresponds to about $5 \mu\text{K}$. The power dissipated in the thermometer was $0.5 \mu\text{W}$.

By use of this calorimeter, we have performed high

resolution heat capacity measurements in the vicinity of phase transition of $\text{SnCl}_2 \cdot 2\text{H}_2\text{O}$,¹²⁾ $\text{SnCl}_2 \cdot 2\text{D}_2\text{O}$ ¹⁸⁾ and Rochelle salt.¹⁹⁾ The imprecision in these measurements was about 0.05%. The accuracy was also found to be satisfactorily high since it was found that the high resolution data agreed closely with those obtained by the ordinary measurement where the latter is available.

References

- 1) L. P. Kadanoff, W. Götze, D. Hamblen, R. Hecht, E.A.S. Lewis, V. V. Palciauskas, M. Rayl, J. Swift, D. Aspnes, and J. Kane, *Rev. Mod. Phys.*, **39**, 395 (1967).
- 2) H. E. Stanley, "Introduction to Phase Transitions and Critical Phenomena," Oxford University Press, London (1971).
- 3) M. J. Buckingham and W. M. Fairbank, "Progress in Low Temperature Physics," Vol. 13, ed. by C.J. Gorter, North Holland, Amsterdam (1961), p. 80.
- 4) A. V. Voronel, S. R. Garber, and V. M. Mamnitskii, *Zh. Eksp. Teor. Fiz.*, **55**, 2017 (1968).
- 5) F. J. Cook, *J. Phys. Chem. Ref. Data*, **2**, 11 (1973).
- 6) W. Reese and L. F. May, *Phys. Rev.*, **162**, 510 (1967); *ibid.*, **167**, 504 (1968); *ibid.*, **181**, 905 (1969).
- 7) P. Schwartz, *Phys. Rev.*, **B4**, 920 (1971).
- 8) E. N. Kostina and G. A. Mil'ner, *Sov. Phys. Solid State*, **14**, 2923 (1973).
- 9) I. Hatta and A. Ikushima, *J. Phys. Chem. Solids*, **34**, 57 (1973).
- 10) K. Govindarajan, B. Viswanathan, and E. S. R. Gopal, *J. Chem. Thermodynamics*, **5**, 73 (1973).
- 11) Ya. A. Kraftmakher, *Zh. Prikl. Mekhan. i Tekhn. Fiz.*, **5**, 176 (1962).
- 12) T. Matsuo, M. Tatsumi, H. Suga, and S. Seki, *Solid State Commun.*, **13**, 1829 (1973).
- 13) R. A. Robie and B. S. Hemingway, *Geological Survey Professional Paper 755*, United States Government Printing Office, Washington (1972).
- 14) G. T. Furukawa, R. E. McCosky, and G. J. King, *J. Res. Nat. Bur. Stand.*, **47**, 256 (1951).
- 15) A. G. Cole, J. O. Hutchens, R. A. Robie, and J. W. Stout, *J. Amer. Chem. Soc.*, **82**, 4807 (1960).
- 16) The International Practical Temperature Scale of 1968, *Metrologia*, **5**, 35 (1969).
- 17) V. E. Gorbunov and V. A. Palkin, *Zh. Fiz. Khim.*, **46**, 1625 (1972).
- 18) Read before the 9-th Japanese Calorimetry Conference, Osaka (1973).
- 19) M. Tatsumi, T. Matsuo, H. Suga, and S. Seki, *Proc. Japan Acad.*, **50**, 476 (1974).